Dalton Transactions

COMMUNICATION

View Article Online
View Journal | View Issue

Cite this: *Dalton Trans.*, 2016, **45**, 15298

Received 22nd July 2016,
Accepted 12th September 2016

DOI: 10.1039/c6dt02910h

www.rsc.org/dalton

{[Ir$_3$(cod)$_3$(μ$_3$-S)$_2$](μ$_3$-S)SnCl}$_2$ – a ternary Ir–Sn–S cluster with the iridium atoms in three different chemical environments†

Eliza Leusmann, Eugenie Geringer, Bastian Weinert and Stefanie Dehnen*

Reactions of Sn–S clusters with [IrCl(cod)]$_2$ afforded an Ir–Sn–S cluster with unprecedented topology, {[Ir$_3$(cod)$_3$(μ$_3$-S)$_2$](μ$_3$-S)SnCl}$_2$, in which two [Ir$_3$S$_2$] units and a central [Sn$_2$S$_2$] unit are connected *via* Ir–S and Ir–Sn bonds. Each of the crystallographically independent Ir atoms exhibits a specific chemical environment. Quantum chemical studies shed light on the electronic structure of the multinary cluster and the Ir–Sn bonds.

Multinary metal/non-metal complexes and clusters have been actively investigated by chemists and physicists as they often combine structural and physical characteristics of the formally underlying binary components, and thus allow for further fine-tuning of respective properties.[1,2] Additionally, the combination of functional organic ligand shells with multinary inorganic cores, opens the field for development of opto-electronics or solar cells components.[3] Polyoxometalates and compounds with group 14/16 elemental combination are intensively investigated working horses in this area.[4,5]

Tetrelchalcogenide T–E and related M–T–E clusters (M = transition metal, T = tetrel, E = chalcogen) combine promising properties in (opto-)electronics or magnetism with structural diversity.[6] The attachment of organic substituents on the surface of such clusters further enhances the diversity. This way, the formation of ternary clusters can also occur *via* metal atom capturing by suitable ligand donor pockets, *e.g.*, upon terminating the organic ligands with chelating groups, to form M@T–E clusters,[7] or aromatic ligands.[8]

So far, the double-decker-shaped cluster [(R^{1}Sn)$_4$S$_6$] (**A**; R^1 = CMe$_2$CH$_2$COMe)[9] has been the most intensely investigated precursor species among all organo-functionalized T–E aggregates. The terminal keto group at its organic moiety R^1 readily reacts with various hydrazines, hydrazones or hydrazides.[5c,10]

Another extension of the Sn–S starting complexes is realized *via* reactions with transition metal complexes ML$_n$X$_m$ (L = ligand, X = halide) to form clusters with ternary inorganic M–T–E cluster cores and reactive organic ligand shells. In most cases so far, coinage metal or Zn atoms were combined this way with T–E units.[7,8c,e,10c]

Other M–T–E elemental combinations remained rare so far, and were approached *via* different routes. For example, the ferrocenyl(Fc)-decorated, adamantane-shaped cluster [(FcSn)$_4$S$_6$] was transferred into the multinary cluster anion [(FcSn)$_8$Ni$_3$S$_{16}$]$^{2-}$ by reaction with [Ni(acac)$_2$] (acac: acetylacetonate).[11] The reaction of compounds that comprise larger cluster moieties, such as the organo-funtionalized [Sn$_6$S$_{10}$] unit,[9a] with transition metal compounds have not been reported yet. A hint towards their reaction potential was, however, suggested by the fact that a series of [(R^{bispy}Sn)$_4$S$_{10}$Zn$_8$X$_8$] clusters (R^{bispy} = CMe$_2$CH$_2$C(Me)NNC(2-py)$_2$; X = Cl, Br, I), obtained from **A** *via in situ*-functionalization with bispyridyl groups and reaction with ZnX$_2$, co-crystallized with [(R^{bispy}Sn)$_4$Sn$_2$S$_{10}$].[7] The latter, however, could not be detected in solution.

We herein present the formation of a cluster with an Ir–Sn–S core, which was synthesized in reactions of [Ir(cod)Cl]$_2$ (cod: 1,5-cyclooctadiene), either by use of **A** or a larger cluster that was obtained upon reaction of **A** with (*E*)-6-(1-hydrazonoethyl)-2,2′-bipyridine (**1**, bipy), [(R^{bipy}Sn)$_4$Sn$_2$S$_{10}$] (**2**, R^{bipy}: CMe$_2$CH$_2$C(Me)=N–N=C(Me)(C$_5$H$_3$N–C$_5$H$_4$N)). **A** was prepared according to the literature.[9] **1** and **2** were synthesized according to similar procedures published recently.[8b] The final product of these reactions, {[Ir$_3$(cod)$_3$(μ$_3$-S)$_2$](μ$_3$-S)SnCl}$_2$ (**3**), is based on two [Ir$_3$S$_2$] units and a central [Sn$_2$S$_2$] unit, which are connected *via* Ir–S and Ir–Sn contacts (Scheme 1). Details of the characterization of the title compounds are to be found in the ESI.†

According to X-ray diffraction analyses,‡ colorless bars of compound **2** crystallize in the monoclinic space group *P*2$_1$/*c*

Fachbereich Chemie and Wissenschaftliches Zentrum für Materialwissenschaften (WZMW), Philipps-Universität Marburg, Hans-Meerwein-Straße 4, D-35043 Marburg, Germany. E-mail: dehnen@chemie.uni-marburg.de; Fax: +49 6421 2825653; Tel: +49 6421 2825751

†Electronic supplementary information (ESI) available: Details of syntheses, single crystal X-ray diffraction, energy-dispersive X-ray (EDX) spectroscopy, micro X-ray fluorescence analysis (μ-RFA), electrospray-ionization mass spectrometry (ESI-MS), and quantum chemical investigation using density functional theory (DFT) methods. CCDC 1446774 and 1446775. For ESI and crystallographic data in CIF or other electronic format see DOI: 10.1039/c6dt02910h

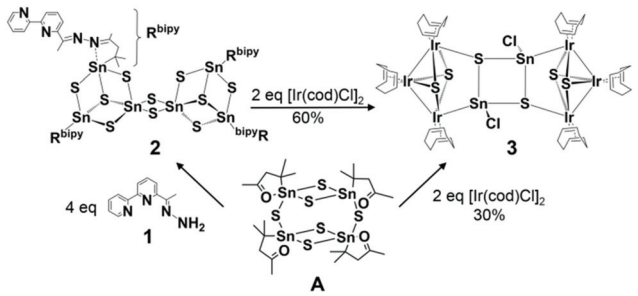

Scheme 1 Formation of compounds **2** and **3** starting from **A**. The "detour" *via* **2** leads to improved crystal yield and quality for X-ray diffraction.†

(a = 10.8761(2) Å, b = 38.3489(7) Å, c = 10.6185(2) Å, β = 94.92(3)°, V = 4412.51(14) Å^3, Z = 2). The molecular structure of **2** (Fig. 1) is based on the known $[Sn_6S_{10}]$ skeleton, hence comprises two doubly μ-S-bridged $[\{(RSn)_2Sn\}S_4]$ defect-heterocubane units. As previously reported for other aromatic molecules and other bulky hydrazine derivatives,[7,8b,9a,12] the inorganic core undergoes a rearrangement from the $[Sn_4S_6]$ unit in **A** to the $[Sn_6S_{10}]$ architecture in **2**. The intramolecular N → Sn coordination and the corresponding $SnS_3C\cdots N$ coordination environment was retained for four of the six Sn atoms during the rearrangement, whereas two Sn atoms adopt an SnS_5 coordination in **2**. All Sn atoms, however, are found in a fivefold coordination and a distorted trigonal bipyramidal coordination geometry. The N atoms of the pyridine rings direct into opposite directions, as they remain uncoordinated. All structural parameters within the inorganic cluster core and the ligand environment are in the common ranges (see ESI†).

However, in contrast to all clusters with the same inorganic scaffold, the chosen conditions recording the ESI(+) mass spectrum of a solution of single crystals of **2** in CH_2Cl_2 (Fig. S4†) comprises the mass cluster of the whole molecule for the first time, as $\{[(R^{bipy}Sn)_4Sn_2S_{10} + 2Na]^{2+}\}_{0.5}$, beside signals of the defect-heterocubane $[(R^{bipy}Sn)_3S_4]^+$ fragment. Previously, only clusters of the latter type were detected. Although one certainly has to handle and interpret mass spectra with great care, as the results depend in part on the measurement conditions, we would like to state that this can be taken at least as a hint towards restricted stability of the larger assembly. Additionally an exact half of the cluster in **2** was observed, as $[(R^{biby}Sn)_2SnS_5 + Na]^+$. With caution, we suggest that the chelating ligands perform a nucleophilic attack on the "inorganic" Sn atoms, thereby replacing one of the bridging S^{2-} ligands each. This initiates the break of the cluster into halves, releasing the $[(RSn)_2SnS_5]$ units. The very poor solubility of **2** inhibited further solution analyses, such as NMR studies.

Conversion of the solution of **2** with two equivalents of $[Ir(cod)Cl]_2$ dissolved in CH_2Cl_2 (stirring for 16 h, filtering and layering with toluene, waiting for two months) leads to the formation of $\{[Ir_3(cod)_3(\mu_3\text{-}S)_2](\mu_3\text{-}S)SnCl\}_2\cdot 2CH_2Cl_2$ (**3**·2CH_2Cl_2). Notably, in both cases the organic ligands were released, retaining only "inorganic" Sn atoms, whereas the COD ligands remained at the Ir atoms. Fig. 2 shows the molecular structure of **3**.

According to X-ray diffraction analyses,‡ black rhombic plates of **3**·2CH_2Cl_2 crystallize in the triclinic space group $P\bar{1}$ (a = 10.130(4) Å, b = 10.979(4) Å, c = 13.757(4) Å, α = 108.21(2)°, β = 89.91(3)°, γ = 90.32(3)°, V = 1453.3(9) Å^3, Z = 1).‡ The cluster comprises an inversion center and is thus composed of two identical subunits. In these, three Ir atoms, an Sn and an S atom form a planar five-membered ring. The three Ir atoms are μ_3-bridged by two further S atoms, generating a distorted square pyramid with a $[Ir_2S_2]$ base and an apical Ir atom. The $[Ir_2S_2]$ four-membered ring is neither rectangular (Ir1–S(1,2)–

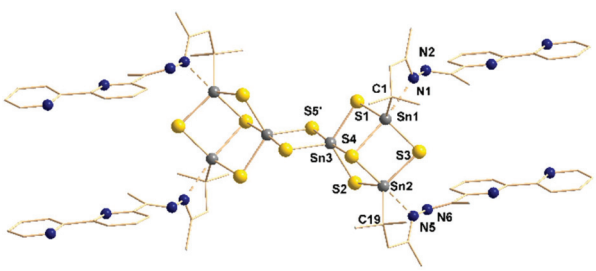

Fig. 1 Molecular structure of $[(R^{bipy}Sn)_4Sn_2S_{10}]$ (**2**) with R^{bipy}: $CMe_2CH_2C(Me)$═N–N═$C(Me)(C_5H_3N–C_5H_4N)$. Grey: Sn, yellow: S, blue: N. C atoms are drawn as wires. H atoms are omitted for clarity. Structural parameters are provided in the ESI.†

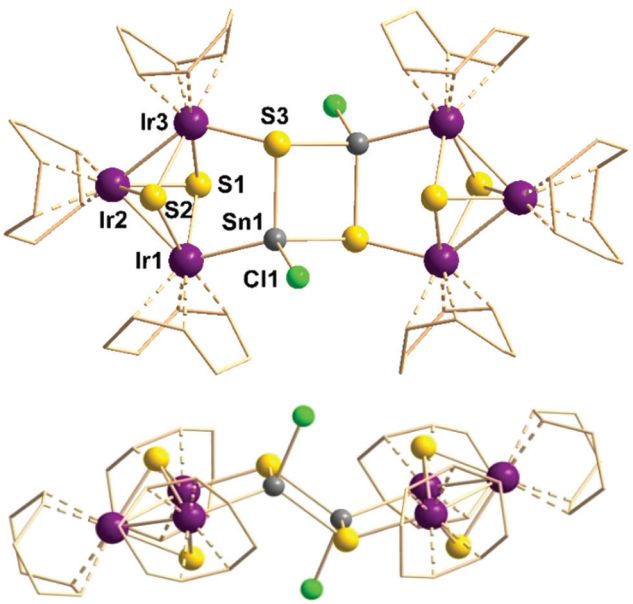

Fig. 2 Molecular structure (top and side view) of **3**. Grey: Sn, yellow: S, green: Cl, violet: Ir atoms. The COD ligands are shown as wires. Selected structural parameters [Å/°]: Ir(1,3)–S(1,2) 2.359(8)–2.417(8), Ir2–S(1,2) 2.318(8)–2.338(8), Ir3–S3 2.445(7), Ir1–Sn1 2.556(3), Sn1–S(3,3′) 2.484(7)–2.513(7), Sn1–Cl1 2.380(8); Ir1–Ir2–Ir3 80.24(6), Ir1–S(1,2)–Ir3 97.3(3)–98.7(2), S1–Ir–S2 78.5(3)–81.5(3), Ir1–Sn1–S3 107.39(18), Ir1–Sn1–S3′ 121.2(2), Ir3–S3–Sn1 98.2(3), Ir3–S3–Sn1′ 122.1(3), Ir1–Sn1–Cl1 118.4(2), S3–Sn1–Cl1 104.2(3)–107.3(2), Sn1–S3–Sn1 85.9(2), S3–Sn1–S3 94.1(2). Further data is provided in the ESI.†

Ir3 angles 97.3(3)° and 98.7(2)°, S1–Ir(1,3)–S2 angles 78.5(3)° and 71.5(3)°) nor planar, but folded about the Ir···Ir axis by 153°, and by 157° about the S···S axis. Still, the deviation from a trigonal bipyramid is larger, with two closer Ir–Ir distances (Ir1–Ir2 2.7840(19) Å, Ir2–Ir3 2.801(2) Å) beside a notably larger Ir1···Ir3 distance (3.599(2) Å). Each Ir atom bears one COD ligand and each Sn atom possesses a terminal chloride ligand, giving the latter a tetrahedral coordination environment (including the Ir–Sn contact). The coordination number and geometry of the Ir atoms is not easily gathered and will be discussed below. The complete cluster is formed by combining the two subunits *via* a central $[Sn_2S_2]$ four-membered ring. The side view (Fig. 2, bottom) indicates a zig-zag arrangement of the two five-membered $[Ir_3SnS]$ rings and the central $[Sn_2S_2]$ unit, with a dihedral angel of 123.4° between the mean planes.

The elemental combination of Ir and Sn is known from intermetallic phases, which exist as $IrSn_2$ (Ir–Sn 2.744 Å),[13a] Ir_3Sn_7 (Ir–Sn): 2.744–2.762 Å),[13b] and $IrSn_4$ (Ir–Sn 2.744–2.748 Å).[13c] Direct Ir–Sn contacts have been also observed in several molecular complexes or clusters, for instance $[Ir@Sn_{12}]^{3-}$ (Ir–Sn 2.8828(5)–2.9414(5) Å), $[Ir(cod)Sn_9]^{3-}$ (Sn–Ir 2.746(2)–2.788(7) Å),[14a] $[Ir(C_7H_8)(PMe_3Ph)_2(SnCl_3)]$ (Ir–Sn 2.5867(6) Å),[14b] $[Ir(CO)_3(PCy_3)(SnPh_3)]$ (Cy: cyclohexyl; Ir–Sn 2.6610(3) Å),[14c] $[Ir(CO)_3(SnPh_3)_2]^-$ (Ir–Sn 2.628(4) Å),[14d] $[\{Ir(CO)_2\}(SnPh_2)_3Bi]$ (Ir–Sn 2.659(14) Å),[14e] $[Ir_2(cod)_2(SnCl_3)_2Cl_2(\mu\text{-}Cl)_2]$ (Sn–Ir 2.578(4) Å),[14f] $[MeSi\{SiMe_2N(p\text{-tol})\}_2\{SiMe_2N(2\text{-}C_6H_3\text{-}4\text{-}CH_3)\}SnIr(cod)(H)(PPh_3)]$ (*p*-tol: 4-methylphenyl; Sn–Ir 2.5798(8) Å),[14g] or $[Ir(CO)_2(SnB_{11}H_{11})_3]^-$ (Ir–Sn 2.571(5)–2.623(5) Å).[14h]

Except the quoted intermetalloid cluster with an Ir atom embedded inside an Sn_{12} cluster shell and the $[Ir(cod)Sn_9]^{3-}$ *closo* cluster, all of the known compounds comprise SnX_nR_{x-n} (X = halide, O, N; R = alkyl, aryl; n = 0–3, x = 1–4) or stannaborate groups as terminal or μ-bridging ligands. In contrast, both Ir and Sn atoms are part of a heterobimetallic metal chalcogenide cluster core in **3**, which is the first one with this elemental combination. The Ir–Sn bond length (2.556(3) Å) is shorter than any of the reported ones, indicating a stronger bonding interaction.

To gain a further insight into the bonding situation, in particular for elucidating the coordination situation of the Ir and Sn atoms, we performed quantum chemical studies using DFT methods within the program package TURBOMOLE.§[15] Besides simultaneous optimizations of the geometric and the electronic structures (on the basis of the single-crystal structural data), we analyzed the atomic orbital (AO) contributions to molecular orbitals (MOs) by means of Mulliken population analyses.[16] As typical for DFT studies, all bond lengths were calculated slightly longer in comparison with the experimental values. Deviations amount to 0.092 Å (Ir–Sn), 0.074–0.079 Å (Ir–Ir), 0.009–0.046 Å (Ir–S), 0.056–0.071 Å (Sn–S), or 0.052 Å (Sn–Cl). These relatively small deviations thus allow for the discussion of the electronic and consequently the bonding situation.

The overall charge of all carbon and all hydrogen atoms is −0.14, emerging from Mulliken population analysis and therefore close to zero. Accordingly, the charge of the inorganic core sums up to an only slightly positive Mulliken charge of +0.14: Ir1 +0.22, Ir2 +0.11, Ir3 +0.64 and Sn1 +0.73 −negative Mulliken charge: S1 −0.41, S2 −0.43, S3 −0.44 and Cl −0.36. Since the charges of both parts, organic shell and inorganic core, are close to zero, a separate observation of the core is acceptable. The Mulliken charges roughly reflect the typical formal oxidation states of the heavy atoms that add up to zero in the sum: six Ir(+I), six S(−II), two Cl(−I) and two Sn(+IV). However, it is quite evident that the values calculated for the three Ir atoms are all different, which reflects the different coordination environments. Given that Ir2 behaves like a "normal" Ir(+I) atom, with a *pseudo*-square pyramidal environment as typical for the d^8 configuration (disregarding the Ir–Ir bonds), one might assign Ir3, with one additional sulfide ligand, a +II oxidation state. Ir1 would be in the same situation with an Sn neighbor instead of the sulfide ligand, and likewise, Sn1 would be in the +IV oxidation state with only electronegative ligands around. Hence, due to similar electronegativities of Sn (1.72) and Ir (1.55),[17] the Ir–Sn bond can be interpreted as to reduce the formal oxidation state of both atom by one number, leading to a formal oxidation state of +I for Ir1 and +III for Sn1 – in accordance with the found Mulliken charges – and to a balanced situation in the sum. However, the Ir–Ir contacts cannot be neglected, which indicates that the picture of formal oxidation states is not useful here, as that the charge differences are much more subtle.

To better illustrate the bonding interactions between Ir1 and Sn1 and within the Ir–Ir–Ir unit, we thus inspected the canonical MOs that indicate both localized and delocalized electron density within the cluster. Several MOs show (moderate) contributions to a direct Ir–Sn interaction, (MOs 193a, 194a, 239a, 270a). One also identifies p-type and d-type cluster orbitals for the $[Ir_3S_2]$ subunits (160a, 161a, 125a, 126a, 130a–132a, 133a, 136a), which are mainly S-mediated (see ESI†). An even clearer picture is observed upon localization of the MOs by using Boys' method,[18] and inspection of the resulting localized MOs (LMOs). Two representative LMOs are shown in Fig. 3.

The LMOs suggest interpreting the Ir–Sn contacts as two-center-two-electron bonds (LMOs 313 and 314, Fig. 3 left), and also the Ir–Ir contacts as essentially two-center-two-electron interactions, with slight contributions of the two apical μ_3-S atoms (LMOs 315–318, Fig. 3, right).

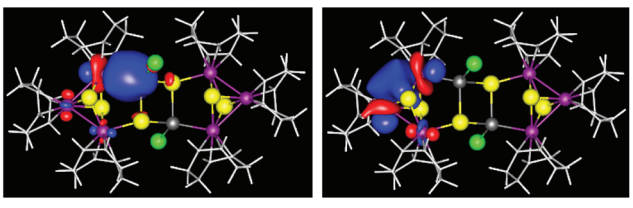

Fig. 3 Localized molecular orbitals (LMOs) of the calculated cluster molecule in **3**, indicating metal–metal bonding. Left: Bonding Ir–Sn contact (LMO 314; equivalent to 313). Right: (S-mediated) Ir–Ir contact (LMO 317; equivalent to 315, 316, 318). Color code according to Fig. 2.

In summary, we have presented two synthetic accesses to the first Ir–Sn–S cluster starting from organotin sulfide clusters. We have determined its crystal structure and elucidated the electronic situation, which indicates rather localized Ir–Sn bonds, whereas the Ir–Ir interactions are incorporated into $[Ir_3S_2]$ cluster bonding.

Notes and references

‡X-ray crystallographic data for CCDC 1446774 (**2**) and 1446775 (**3**): data collection on a STOE IPDS2 diffractometer using graphite-monochromatized Mo Kα radiation (λ = 0.71073 Å) at 100 K. Structure solution and refinement by direct methods and fullmatrix least-squares on F^2, respectively; SHELX and Olex software.[19] The crystallographic data are provided in the ESI.† This work was financially supported by the Deutsche Forschungsgemeinschaft (DFG) within the frameworks of GRK 1782 and SFB 1083.

§Density functional theory (DFT) calculations were done with the program system TURBOMOLE[15a] employing the Becke-Perdew 86 (BP86) functional[15b,c] with def2-TZVP bases[15d] and respective fitting bases[15e] for the evaluation of the Coulomb matrix. Effective core potentials (ECPs) were used for Sn and Ir atoms (ECP-28 and ECP-60).[15f,g] Contour plots were generated with gOpenMol.[16b]

1 (*a*) C. B. Khadka, A. Eichhöfer, F. Weigend and J. F. Corrigan, *Inorg. Chem.*, 2012, **51**, 2747; (*b*) C. Xu, J.-J. Zhang, Q. Chen, T. Duan, W.-H. Leung and Q.-F. Zhang, *Inorg. Chem. Commun.*, 2012, **21**, 1; (*c*) A. Eichhöfer, J. Olkowska-Oetzel, D. Fenske, K. Fink, V. Mereacre, A. K. Powell and G. Buth, *Inorg. Chem.*, 2009, **48**, 8977; (*d*) S. Dehnen and M. Melullis, *Coord. Chem. Rev.*, 2007, **251**, 1259; (*e*) J. Heine and S. Dehnen, *Z. Anorg. Allg. Chem.*, 2012, **638**, 2425.

2 (*a*) D. Aldakov, A. Lefrançois and P. Reiss, *J. Mater. Chem. C*, 2013, **1**, 3756.

3 S. V. Kershaw, A. S. Susha and A. L. Rogach, *Chem. Soc. Rev.*, 2013, **42**, 3033.

4 A. Proust, B. Matt, R. Villanneau, G. Guillemot, P. Gouzerh and G. Izzet, *Chem. Soc. Rev.*, 2012, **41**, 7605.

5 (*a*) M. Wagner, T. Zöller, W. Hiller, M. H. Prosenc and K. Jurkschat, *Chem. Commun.*, 2013, **49**, 8925; (*b*) M. Bouška, L. Střižík, L. Dostál, A. Růžička, A. Lyčka, L. Beneš, M. Vlček, J. Přikryl, P. Knotek, T. Wágner and R. Jambor, *Chem. – Eur. J.*, 2013, **19**, 1877; (*c*) B. E. K. Barth, B. A. Tkachenko, J. P. Eußner, P. R. Schreiner and S. Dehnen, *Organometallics*, 2014, **33**, 1678.

6 (*a*) P. Feng, X. Bu and N. Zheng, *Acc. Chem. Res.*, 2005, **38**, 293; (*b*) M. G. Kanatzidis, *Adv. Mater.*, 2007, **19**, 1165; (*c*) D. G. MacDonald and J. F. Corrigan, *Philos. Trans. R. Soc. London, Ser. A*, 2010, **368**, 1455.

7 B. E. K. Barth, E. Leusmann, K. Harms and S. Dehnen, *Chem. Commun.*, 2013, **49**, 6590.

8 (*a*) B. Barth, K. Harms and S. Dehnen, *Eur. J. Inorg. Chem.*, 2014, 2406; (*b*) E. Leusmann, F. Schneck and S. Dehnen, *Organometallics*, 2015, **34**, 3264; (*c*) E. Leusmann, M. Wagner, N. W. Rosemann, S. Chatterjee and S. Dehnen, *Inorg. Chem.*, 2014, **53**, 4228; (*d*) Z. You, K. Harms and S. Dehnen, *Eur. J. Inorg. Chem.*, 2015, 5322; (*e*) Z. You, J. Bergunde, B. Gerke, R. Pöttgen and S. Dehnen, *Inorg. Chem.*, 2014, **53**, 12512; (*f*) Z. You, R. Möckel, J. Bergunde and S. Dehnen, *Chem. – Eur. J.*, 2014, **20**, 13491; (*g*) Z. You and S. Dehnen, *Inorg. Chem.*, 2013, **52**, 12332; (*h*) Z. You, D. Fenske and S. Dehnen, *Dalton Trans.*, 2013, **42**, 8179.

9 (*a*) Z. Hassanzadeh Fard, L. Xiong, C. Müller, M. Hołyńska and S. Dehnen, *Chem. – Eur. J.*, 2009, **15**, 6595; (*b*) Z. Hassanzadeh Fard, C. Müller, T. Harmening, R. Pöttgen and S. Dehnen, *Angew. Chem., Int. Ed.*, 2009, **48**, 4441.

10 (*a*) N. Rinn, J. P. Eußner, W. Kaschuba, X. Xie and S. Dehnen, *Chem. – Eur. J.*, 2016, **22**, 3094; (*b*) J. P. Eußner, R. O. Kusche and S. Dehnen, *Chem. – Eur. J.*, 2015, **21**, 12376; (*c*) J. Eußner and S. Dehnen, *Chem. Commun.*, 2014, **50**, 11385; (*d*) J. P. Eußner, B. E. K. Barth, E. Leusmann, Z. You, N. Rinn and S. Dehnen, *Chem. – Eur. J.*, 2013, **19**, 13792; (*e*) J. P. Eußner and S. Dehnen, *Z. Anorg. Allg. Chem.*, 2012, **638**, 1827; (*f*) S. Heimann, M. Holynska and S. Dehnen, *Chem. Commun.*, 2011, **47**, 1881; (*g*) M. R. Halvagar, Z. Hassanzadeh Fard and S. Dehnen, *Chem. – Eur. J.*, 2011, **17**, 4371; (*h*) M. R. Halvagar, Z. Hassanzadeh Fard and S. Dehnen, *Chem. Commun.*, 2010, **46**, 4716; (*i*) Z. Hassanzadeh Fard, M. R. Halvagar and S. Dehnen, *J. Am. Chem. Soc.*, 2010, **32**, 2848; (*j*) M. R. Halvagar, Z. Hassanzadeh Fard and S. Dehnen, *Inorg. Chem.*, 2009, **48**, 7373.

11 C. Pöhlker, I. Schellenberg, R. Pöttgen and S. Dehnen, *Chem. Commun.*, 2010, **46**, 2605.

12 Z. Hassanzadeh Fard, M. R. Halvagar and S. Dehnen, *J. Am. Chem. Soc.*, 2010, **132**, 2848.

13 (*a*) H. Nowotny, K. Schubert and U. Dettinger, *Metallforschung*, 1946, **1**, 137; (*b*) M. Schlüter, U. Häussermann, B. Heying and R. Pöttgen, *J. Solid State Chem.*, 2003, **173**, 418; (*c*) E. L. Nordmark, O. Wallner and U. Häussermann, *J. Solid State Chem.*, 2002, **168**, 34.

14 (*a*) J.-Q. Wang, S. Stegmaier, B. Wahl and T. F. Fässler, *Chem. – Eur. J.*, 2010, **16**, 1793; (*b*) M. R. Churchill and K.-K. G. Lin, *J. Am. Chem. Soc.*, 1974, **96**, 76; (*c*) M. A. Esteruelas, F. J. Lahoz, M. Olivan, E. Onate and L. A. Oro, *Organometallics*, 1994, **13**, 4246; (*d*) J. M. Allen, W. W. Brennessel, C. E. Buss, J. E. Ellis, M. E. Minyaev, M. Pink, G. F. Warnock, M. L. Winzenburg and V. G. Young, *Inorg. Chem.*, 2001, **40**, 5279; (*e*) R. D. Adams, M. Chen, G. Elpitiya and Q. Zhang, *Organometallics*, 2012, **31**, 7264; (*f*) J. Choudhury, S. Podder and S. Roy, *J. Am. Chem. Soc.*, 2005, **127**, 6162; (*g*) M. Kilian, H. Wadepohl and L. H. Gade, *Organometallics*, 2008, **27**, 524; (*h*) S. Fleischhauer, K. Eichele, I. Schellenberg, R. Pöttgen and L. Wesemann, *Organometallics*, 2011, **30**, 3200.

15 (*a*) Turbomole Version 6.6, © Turbomole GmbH 2011. Turbomole is a development of University of Karlsruhe and Forschungszentrum Karlsruhe 1989–2007, Turbomole GmbH since 2007; (*b*) A. D. Becke, *Phys. Rev. A*, 1988, **38**, 3098; (*c*) J. P. Perdew, *Phys. Rev. B: Condens. Matter*, 1986, **33**, 8822; (*d*) F. Weigend and R. Ahlrichs, *Phys. Chem. Chem. Phys.*, 2005, **7**, 3297; (*e*) F. Weigend, *Phys. Chem. Chem. Phys.*, 2006, **8**, 1057; (*f*) M. Dolg, H. Stoll, A. Savin

and H. Preuss, *Theor. Chim. Acta*, 1989, **75**, 173; (*g*) H. Stoll, B. Metz and M. Dolg, *J. Comput. Chem.*, 2002, **23**, 767.

16 (*a*) R. S. Mulliken, *J. Chem. Phys.*, 1955, **23**, 1833; (*b*) D. L. Bergman, L. Laaksonen and A. Laaksonen, *J. Mol. Graphics Modell.*, 1997, **15**, 301.

17 A. F. Holleman, E. Wiberg and N. Wiberg, *Lehrbuch der Anorganischen Chemie*, Walter de Gruyter, Berlin, 2007.

18 (*a*) S. F. Boys, *Rev. Mod. Phys.*, 1960, **32**, 296; (*b*) J. M. Foster and S. F. Boys, *Rev. Mod. Phys.*, 1960, **32**, 300.

19 (*a*) G. M. Sheldrick, *Acta Crystallogr., Sect. A: Fundam. Crystallogr.*, 2008, **64**, 112; (*b*) G. M. Sheldrick, *SHELXL-2013*, University of Göttingen, Germany, 2013; (*c*) O. V. Dolomanov, L. J. Bourhis, R. J. Gildea, J. A. Howard and H. J. Puschmann, *Appl. Crystallogr.*, 2009, **42**, 339.